

Communication

# The Activating Effect of Strong Acid for Pd-Catalyzed Directed C–H Activation by Concerted Metalation-Deprotonation Mechanism

Heming Jiang<sup>1,2</sup> and Tian-Yu Sun<sup>2,\*</sup> 

<sup>1</sup> Lab of Computational Chemistry and Drug Design, State Key Laboratory of Chemical Oncogenomics, Peking University Shenzhen Graduate School, Shenzhen 518055, China; jiangheming@pku.edu.cn

<sup>2</sup> Shenzhen Bay Laboratory, Shenzhen 518132, China

\* Correspondence: Tian-Yu\_Sun@pku.edu.cn

**Abstract:** A computational study on the origin of the activating effect for Pd-catalyzed directed C–H activation by the concerted metalation-deprotonation (CMD) mechanism is conducted. DFT calculations indicate that strong acids can make Pd catalysts coordinate with directing groups (DGs) of the substrates more strongly and lower the C–H activation energy barrier. For the CMD mechanism, the electrophilicity of the Pd center and the basicity of the corresponding acid ligand for deprotonating the C–H bond are vital to the overall C–H activation energy barrier. Furthermore, this rule might disclose the role of some additives for C–H activation.

**Keywords:** directed C–H activation; concerted metalation–deprotonation mechanism; acid effect; electrophilicity; basicity



**Citation:** Jiang, H.; Sun, T.-Y. The Activating Effect of Strong Acid for Pd-Catalyzed Directed C–H Activation by Concerted Metalation-Deprotonation Mechanism. *Molecules* **2021**, *26*, 4083. <https://doi.org/10.3390/molecules26134083>

Academic Editor: Antonio Massa

Received: 8 June 2021

Accepted: 1 July 2021

Published: 4 July 2021

**Publisher's Note:** MDPI stays neutral with regard to jurisdictional claims in published maps and institutional affiliations.



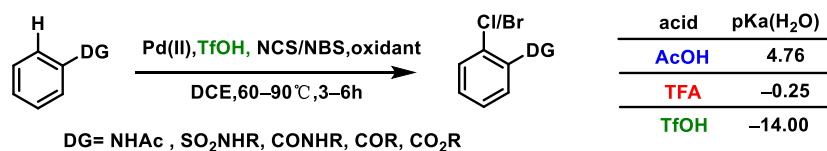
**Copyright:** © 2021 by the authors. Licensee MDPI, Basel, Switzerland. This article is an open access article distributed under the terms and conditions of the Creative Commons Attribution (CC BY) license (<https://creativecommons.org/licenses/by/4.0/>).

## 1. Introduction

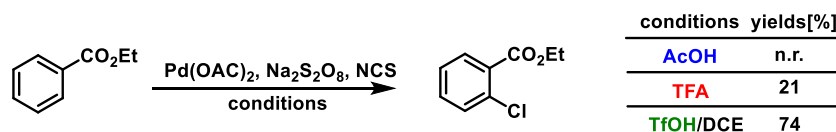
Transition metal-catalyzed C–H activation to synthesize diverse organic molecules from simple hydrocarbon derivatives has emerged as a powerful tool for C–C and C–heteroatom bond formation and has received significant attention in recent years [1–7]. However, regioselectivity and reactivity have remained the most significant challenges in this active research field. Therefore, different strategies, especially directed C–H activation strategies, have been developed to improve regioselectivity and reactivity for C–H activation [8–21]. The directing groups (DGs) on substrates can chelate the metal catalyst and guide it to a specific position. Strong coordinating DGs usually contain strongly coordinating atoms, such as nitrogen, phosphorus, or sulfur atoms. They could widely promote C–H activation functionalization [22–24]. However, strong coordinating DGs are challenging to remove from the final products, limiting the utility of this strategy. Weak coordinating DGs (e.g., ketones, carboxylic acids, and ethers) are commonly occurring functional groups on the substrates and usually have much lower reactivity for C–H activation reaction [25–30]. Yu and co-workers have established several strategies to overcome the low reactivity of C–H activation by weak coordination, such as using counter cation effect, auxiliaries and monoprotected amino acid ligands [31–35]. Although impressive progress has been made, the scope of application of these strategies is still limited [36,37]. Using strong acid is also a widely used strategy to promote C–H activation; for example, palladium(II)-catalyzed ortho-selective C–H chlorination/bromination has demonstrated that proper strong acids (TFA, TfOH) could promote the reactivity of ortho-selective C–H bond cleavage (Schemes 1 and 2) [25–30,38–40]. These experimental results showed that higher catalytic activity occurred in reactions with lower pKa value acids.

The activating effect of a strong acid on Pd(II)-Catalyzed directed C–H activation has been known for a long time. Many kinds of C–H functionalization can be promoted by TFA or TfOH, such as carboxylation, [41] olefination, [42] arylation, [43,44] fluorination, [45] carbonylation, [46] trifluoromethylation, [47] amidation, [48] and oxygenation [49,50]. However, current understanding of the nature of strong acid-assisted C–H activation is

still limited [51,52]. Fujiwara proposed that strong acid as a solvent facilitates the generation of highly cationic species ( $[PdX]^+$ ) through ligand exchange (Scheme 3), which are very electrophilic. Cyclopalladium intermediates can be formed through the electrophilic aromatic substitution ( $S_EAr$ ) of the C–H bond [53]. Other researchers have had a similar opinion to Fujiwara regarding the activating effect of strong acid [41–50].



Scheme 1. Corresponding pKa of different acids in ortho-selective C–H bond functionalization.

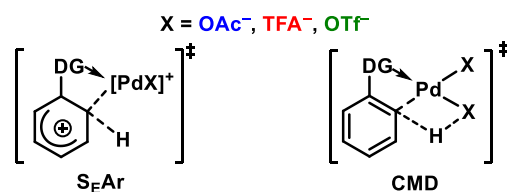


Scheme 2. Corresponding reaction yields of different acids in ortho-selective C–H bond functionalization.



Scheme 3. Ligand exchange process.

Besides  $S_EAr$ , other frequently proposed mechanisms for C–H activation, including oxidative addition,  $\sigma$ -bond metathesis, and CMD mechanism, do not generate cationic species ( $[PdX]^+$ ) [54–59]. The CMD mechanism has been widely accepted as the best pathway for Pd-catalyzed C–H bond cleavage (Scheme 4) [60–65]. Therefore, we carried out density functional theory (DFT) [66] studies to explore the origin of the activating effect of strong acid on Pd-catalyzed directed C–H activation.



Scheme 4. The  $S_EAr$  and CMD mechanism for Pd-catalyzed directed C–H activation.

## 2. Results and Discussion

Since C–H activation is usually involved in the rate-determining step (RDS), [8–50] we hypothesized the relative free energy of transition states of C–H cleavage ( $\Delta G_{TS}^\ddagger$ ) can determine the reactivity. The CMD mechanism was chosen for C–H activation, which usually has the lowest barrier among the frequently proposed mechanisms [57,58]. The transition state for the  $S_EAr$  mechanism could not be located (see Figure S1, Supplementary Materials). Five substrates with different DGs were chosen; these substrates have previously been studied by experiments [38–40,49]. Trimeric  $[Pd(OAc)_2]_3$  was chosen as the reference point of DFT calculations [67–69]. X-ray crystallography has provided evidence that when a strong acid such as TFA or TfOH is used, the OAc<sup>−</sup> in the palladium acetate can be exchanged with TFA<sup>−</sup> or OTf<sup>−</sup> to form  $Pd(TFA)_2$  or  $Pd(OTf)_2$  [48,70–72]. As shown in Figure 1, for all of the five substrates, the  $\Delta G_{TS}^\ddagger$  using three different Pd catalysts is in the same order:  $\Delta G_{TS}^\ddagger[Pd(OTf)_2] < \Delta G_{TS}^\ddagger[Pd(TFA)_2] < \Delta G_{TS}^\ddagger[Pd(OAc)_2]$ . The order of reactivity is consistent with the experimental results, [38–40,73,74] indicating our DFT calculation is reliable.

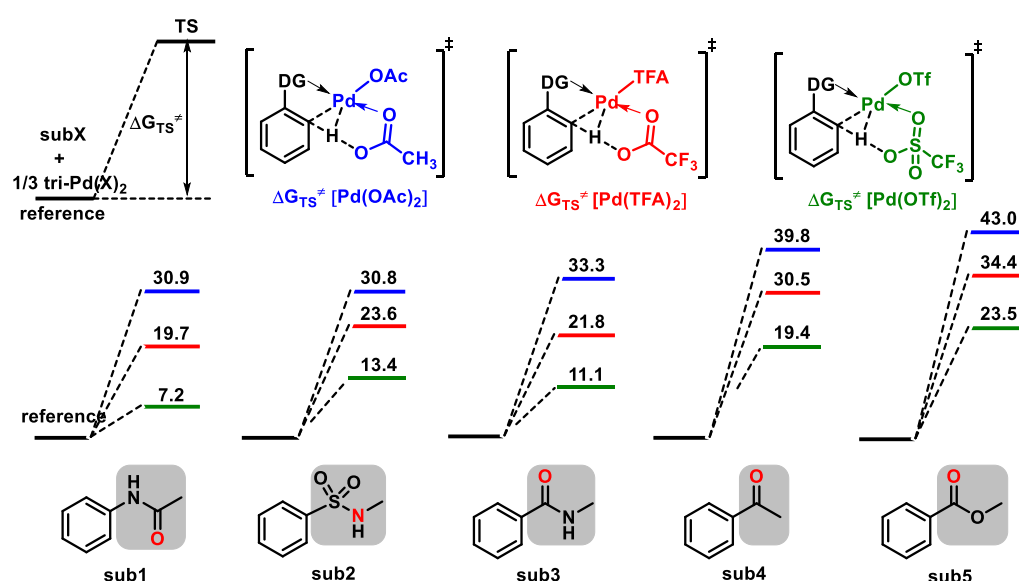
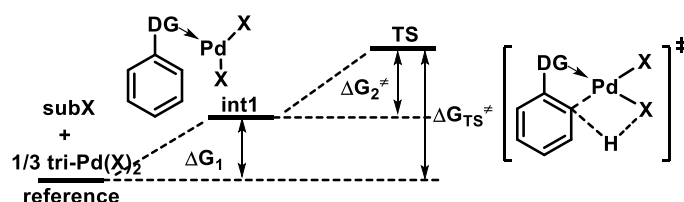


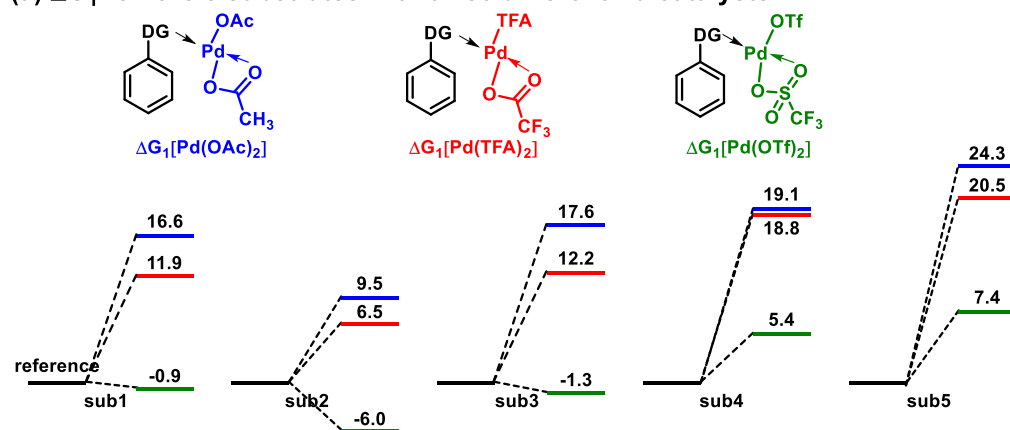
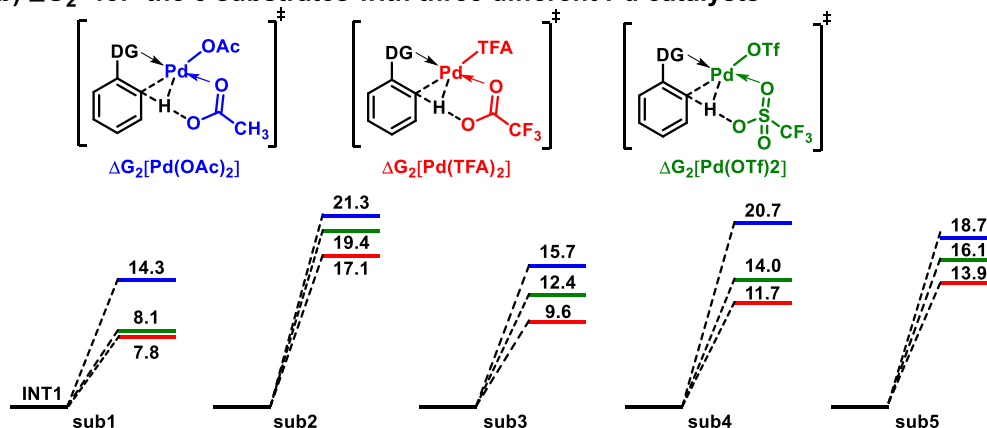
**Figure 1.** Calculated activation free energies by CMD mechanism ( $\Delta G_{TS}^\ddagger$ , kcal/mol) for the five substrates with three different Pd catalysts. The coordination atoms are marked in red.

Next, energy decomposition strategy was used to explore the origin of the activating effect for directed C–H activation by strong acid [63,75–78]. As shown in Scheme 5,  $\Delta G_{TS}^\ddagger$  can be decomposed into two parts:  $\Delta G_1$  and  $\Delta G_2^\ddagger$ .  $\Delta G_1$  is the reaction energy caused by the coordination between the DG and the Pd catalyst.  $\Delta G_2^\ddagger$  represents the energy needed to proceed with the C–H activation from int1. This strategy can reflect how the three different Pd catalysts influence  $\Delta G_1$  and  $\Delta G_2^\ddagger$ , respectively.



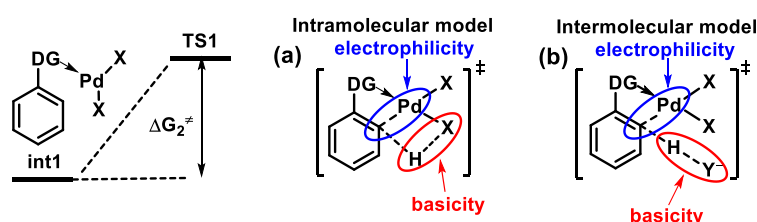
**Scheme 5.**  $\Delta G_{TS}^\ddagger$  can be decomposed into two parts:  $\Delta G_1$  and  $\Delta G_2^\ddagger$ . They represent coordinating energy and C–H activation energy barrier respectively.

For all of the five substrates, the order of  $\Delta G_1$  using the three different Pd catalysts can be summarized as  $\Delta G_1[\text{Pd}(\text{OTf})_2] < \Delta G_1[\text{Pd}(\text{TFA})_2] < \Delta G_1[\text{Pd}(\text{OAc})_2]$  (see Figure 2a), which is in the reverse order of electrophilicity of the Pd catalysts:  $\text{Pd}(\text{OTf})_2 > \text{Pd}(\text{TFA})_2 > \text{Pd}(\text{OAc})_2$  [48]. For  $\Delta G_1$ , the conclusion can be drawn that the more electrophilic Pd catalyst results in better coordination with DGs. For  $\Delta G_2^\ddagger$ , all of the five substrates have the consistent order:  $\Delta G_2^\ddagger[\text{Pd}(\text{TFA})_2] < \Delta G_2^\ddagger[\text{Pd}(\text{OTf})_2] < \Delta G_2^\ddagger[\text{Pd}(\text{OAc})_2]$  (see Figure 2b). The order of  $\Delta G_2^\ddagger$  is different from that of  $\Delta G_1$ , and the C–H activation energy barrier of  $\text{Pd}(\text{TFA})_2$  is the lowest. It was generally believed that a more electrophilic Pd catalyst would result in a lower barrier for the C–H activation step in the past [41–50]. However, our results do not support this belief: the electrophilicity of  $\text{Pd}(\text{OTf})_2$  is strongest, but its C–H activation energy barrier is not the lowest. Therefore, the reason why the C–H activation energy barrier of  $\text{Pd}(\text{TFA})_2$  is the lowest needs further study.

(a)  $\Delta G_1$  for the 5 substrates with three different Pd catalysts(b)  $\Delta G_2^\ddagger$  for the 5 substrates with three different Pd catalysts

**Figure 2.** (a)  $\Delta G_1$  (kcal/mol) for the 5 substrates with three different Pd catalysts; (b)  $\Delta G_2^\ddagger$  (kcal/mol) for the 5 substrates with three different Pd catalysts.

Inspection of the TS by the CMD mechanism demonstrated that  $\Delta G_2^\ddagger$  is related to the metal center's electrophilicity and the basicity of the acid ligand (Scheme 6a). To investigate the influence of electrophilicity and basicity on  $\Delta G_2^\ddagger$  separately, an intermolecular model was built to decompose the effect of the two factors (Scheme 6b).



**Scheme 6.** The electrophilicity of the metal center and the basicity of the acid ligand in the (a) intramolecular model and (b) intermolecular model.

As shown in Figure 3, sub5 was chosen as an example for the intermolecular model study. In each row, the Pd catalyst in the three TSs is the same, but with three different external acid ligands, i.e.,  $\text{OAc}^-$ ,  $\text{TFA}^-$  and  $\text{OTf}^-$ . From each row, we can see how the basicity of acid ligands influences  $\Delta G_2^\ddagger$ . In each column, the external acid ligand in the three TSs is the same, but with three different Pd catalysts, i.e.,  $\text{Pd}(\text{OAc})_2$ ,  $\text{Pd}(\text{TFA})_2$ ,  $\text{Pd}(\text{OTf})_2$ . From each column, we can see how electrophilicity of the Pd catalysts influences  $\Delta G_2^\ddagger$ . The three diagonal transition states, which have the same external acid ligand and the ligand of Pd catalysts, are most similar to our intramolecular mechanism.

For each row, the C–H activation energy barrier of the intermolecular model decreases with increasing basicity of the external acid ligand. The Pd(X)<sub>2</sub>\_OAc transition states have the lowest energy barrier. The energy differences between the OAc<sup>−</sup> and TFA<sup>−</sup> ligands are about 4.6 and 6.3 kcal/mol, and the similar gaps between the TFA<sup>−</sup> and OTf<sup>−</sup> ligands are about 5.6 and 6.8 kcal/mol. For each column, the C–H activation energy barrier of the intermolecular model decreases with the increasing electrophilicity of the Pd catalyst, and the Pd(OTf)<sub>2</sub>\_X transition states have the lowest energy barrier. The energy difference between the Pd(OAc)<sub>2</sub> and Pd(TFA)<sub>2</sub> catalysts is about 13.9–15.8 kcal/mol, much larger than the gap of 2.1–3.1 kcal/mol between the Pd(TFA)<sub>2</sub> and Pd(OTf)<sub>2</sub> catalysts. Therefore, the Pd(OTf)<sub>2</sub>\_OAc transition state with the strongest basicity of the OAc<sup>−</sup> ligand and the strongest electrophilicity of the Pd(OTf)<sub>2</sub> catalyst has the lowest energy barrier among the nine intermolecular models.

However, for the three diagonal transition states with the same external acid ligand and ligand of Pd catalysts, electrophilicity and basicity show an opposite trend. For example, although the electrophilicity of the metal center in Pd(OTf)<sub>2</sub> is the strongest, the basicity of the acid ligand (OTf<sup>−</sup>) is the weakest. The Pd(TFA)<sub>2</sub>\_TFA transition state has the lowest energy barrier considering the influence of the external acid ligand's basicity and the Pd catalyst's electrophilicity, consistent with the lowest C–H activation energy barrier of Pd(TFA)<sub>2</sub> in the intramolecular CMD process. According to the above discussion, it can be concluded that for the CMD mechanism, the electrophilicity of Pd catalysts and the basicity of acid ligands are critical to C–H activation.

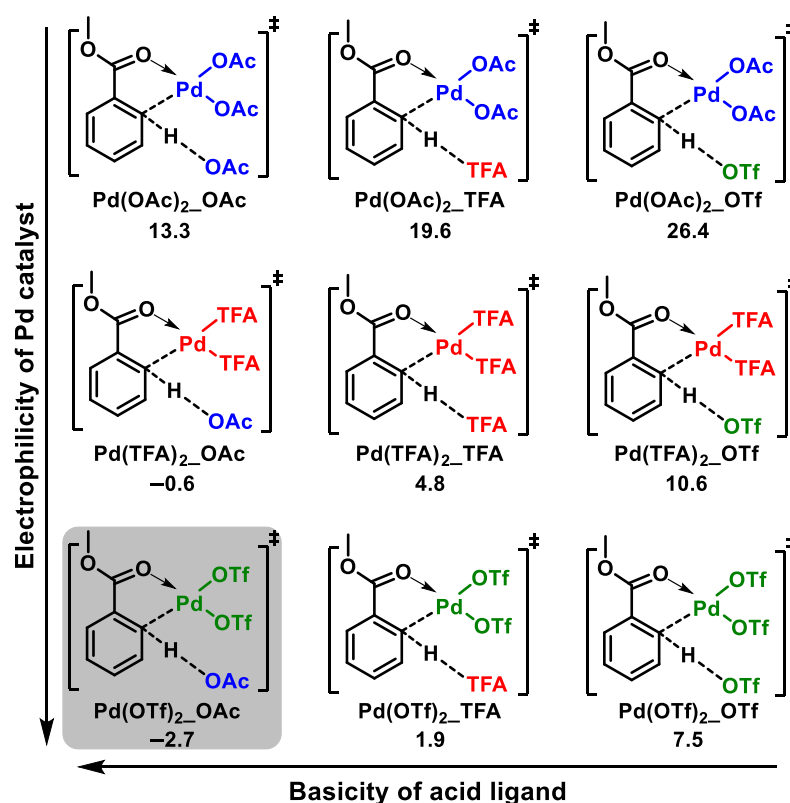


**Figure 3.** The relative free activation energies (kcal/mol) for the intermolecular models of sub5 with three different Pd catalysts and three different anionic external acid ligands (OAc<sup>−</sup>, TFA<sup>−</sup>, TfO<sup>−</sup>).

Inspired by the lowest activation energy of Pd(OTf)<sub>2</sub>\_OAc, we hypothesized that C–H activation via an intermolecular CMD mechanism with a strong electrophilic Pd catalyst and strong external base may be favored, and some experiments support our hypothesis. In Yu's work, the combination of Pd(OTf)<sub>2</sub> and *N*-Methyl-2-pyrrolidone (NMP, a stronger base than TfO<sup>−</sup>) is crucial for C–H fluorination [45]. Our calculations indicate

that the NMP-assistant intermolecular C–H activation process is about 9 kcal/mol lower in energy than the intramolecular C–H deprotonation by  $\text{TfO}^-$  (see Figure 4a). Buchwald and coworkers found that the combination of  $\text{Pd}(\text{OAc})_2/\text{TFA}$  and DMSO can improve the yield of C–H arylation [44]. They proposed that palladium black formation could be slowed by the addition of DMSO (10 mol%). Our calculations indicate that DMSO, a stronger base than  $\text{TFA}^-$ , can also promote intermolecular deprotonation (see Figure 4b). As shown in Figure 4 and Figure S3 (Supplementary Materials), our calculations demonstrated that the intermolecular mechanism is more favorable than the intramolecular mechanism for the above two studies. Our findings might disclose the role of some additives for C–H functionalization.

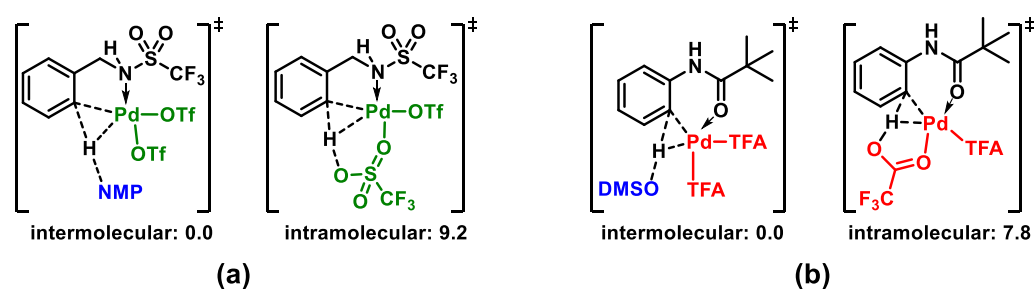


**Figure 4.** Calculated relative activation free energies (kcal/mol) of intermolecular and intramolecular CMD mechanism. Intermolecular models were chosen as the reference point. (a) NMP–assistant process; (b) DMSO–assistant process.

### 3. Conclusions

In summary, the activating effect of strong acid for Pd(II)-catalyzed directed C–H functionalization was investigated with DFT calculations. Our results were consistent with previous experimental results and disclosed that the origin of the activating effect by strong acid comes from two parts:  $\Delta G_1$  (coordination energy between the DG and the Pd catalyst) and  $\Delta G_2^\ddagger$  (C–H activation energy). For the CMD mechanism, the electrophilicity of the Pd center and the basicity of the related acid ligand for deprotonation of the C–H bond is vital to the overall C–H activation energy barrier. This rule can be used to explain the role of some additives for C–H activation. It is hoped that our study could be used to improve the reactivity of some C–H functionalization reactions.

**Supplementary Materials:** Figure S1: The scan of C–H bond of cationic species ( $[\text{PdOAc}]^+$ ), Figure S2: The relative free energy of different intermediates of sub2, Figure S3: The relative free energy barrier of the intermolecular model.

**Author Contributions:** Computation, data curation, writing—original draft preparation, H.J.; writing—review and editing, supervision, project administration, T.-Y.S.; funding acquisition, H.J. and T.-Y.S. All authors have read and agreed to the published version of the manuscript.

**Funding:** This research was funded by Shenzhen Post-doctoral Special Funding, grant number S219201013 and China Postdoctoral Science Foundation, grant number 8206300344.

**Institutional Review Board Statement:** Not applicable.

**Informed Consent Statement:** Not applicable.

**Data Availability Statement:** More details about DFT calculation are in Supporting Information. This material is available free of charge via the Internet at <http://pubs.acs.org>.

**Conflicts of Interest:** The authors declare no conflict of interest.

**Sample Availability:** Samples of the compounds are not available from the authors.

## References

1. Shilov, A.E.; Shul'pin, G.B. Activation of C–H Bonds by Metal Complexes. *Chem. Rev.* **1997**, *97*, 2879–2932. [[CrossRef](#)] [[PubMed](#)]
2. Daugulis, O.; Do, H.-Q.; Shabashov, D. Palladium- and Copper-Catalyzed Arylation of Carbon–Hydrogen Bonds. *Acc. Chem. Res.* **2009**, *42*, 1074–1086. [[CrossRef](#)] [[PubMed](#)]
3. Lyons, T.W.; Sanford, M.S. Palladium-Catalyzed Ligand-Directed C–H Functionalization Reactions. *Chem. Rev.* **2010**, *110*, 1147–1169. [[CrossRef](#)]
4. Neufeldt, S.R.; Sanford, M.S. Controlling Site Selectivity in Palladium-Catalyzed C–H Bond Functionalization. *Acc. Chem. Res.* **2012**, *45*, 936–946. [[CrossRef](#)]
5. Ackermann, L. Carboxylate-Assisted Ruthenium-Catalyzed Alkyne Annulations by C–H/Het–H Bond Functionalizations. *Acc. Chem. Res.* **2014**, *47*, 281–295. [[CrossRef](#)]
6. Gao, K.; Yoshikai, N. Low-Valent Cobalt Catalysis: New Opportunities for C–H Functionalization. *Acc. Chem. Res.* **2014**, *47*, 1208–1219. [[CrossRef](#)]
7. Gandeepan, P.; Müller, T.; Zell, D.; Cera, G.; Warratz, S.; Ackermann, L. 3d Transition Metals for C–H Activation. *Chem. Rev.* **2019**, *119*, 2192–2452. [[CrossRef](#)] [[PubMed](#)]
8. Phipps, R.J.; Gaunt, M.J. A Meta-Selective Copper-Catalyzed C–H Bond Arylation. *Science* **2009**, *323*, 1593–1597. [[CrossRef](#)]
9. Wang, D.-H.; Engle, K.M.; Shi, B.-F.; Yu, J.-Q. Ligand-Enabled Reactivity and Selectivity in a Synthetically Versatile Aryl C–H Olefination. *Science* **2010**, *327*, 315–319. [[CrossRef](#)]
10. Brückl, T.; Baxter, R.D.; Ishihara, Y.; Baran, P.S. Innate and Guided C–H Functionalization Logic. *Acc. Chem. Res.* **2011**, *45*, 826–839. [[CrossRef](#)]
11. Rousseau, G.; Breit, B. Removable Directing Groups in Organic Synthesis and Catalysis. *Angew. Chem. Int. Ed.* **2011**, *50*, 2450–2494. [[CrossRef](#)]
12. Luo, J.; Preciado, S.; Larrosa, I. Overriding Ortho–Para Selectivity via a Traceless Directing Group Relay Strategy: The Meta-Selective Arylation of Phenols. *J. Am. Chem. Soc.* **2014**, *136*, 4109–4112. [[CrossRef](#)] [[PubMed](#)]
13. Chu, J.C.K.; Rovis, T. Complementary Strategies for Directed C(sp<sup>3</sup>)–H Functionalization: A Comparison of Transition-Metal-Catalyzed Activation, Hydrogen Atom Transfer, and Carbene/Nitrene Transfer. *Angew. Chem. Int. Ed.* **2018**, *57*, 62–101. [[CrossRef](#)] [[PubMed](#)]
14. Dey, A.; Sinha, S.K.; Achar, T.K.; Maiti, D. Accessing Remote meta- and para-C(sp<sup>2</sup>)–HBonds with Covalently Attached Directing Groups. *Angew. Chem. Int. Ed.* **2019**, *58*, 10820–10843. [[CrossRef](#)] [[PubMed](#)]
15. Tang, R.-Y.; Li, G.; Yu, J.-Q. Conformation-induced remote meta-C–H activation of amines. *Nature* **2014**, *507*, 215–220. [[CrossRef](#)]
16. Zhao, C.; Crimmin, M.R.; Toste, F.D.; Bergman, R.G. Ligand-Based Carbon–Nitrogen Bond Forming Reactions of Metal Dinitrosyl Complexes with Alkenes and Their Application to C–H Bond Functionalization. *Acc. Chem. Res.* **2014**, *47*, 517–529. [[CrossRef](#)]
17. Rouquet, G.; Chatani, N. Catalytic Functionalization of C(sp<sup>2</sup>)-H and C(sp<sup>3</sup>)-H Bonds by Using Bidentate Directing Groups. *Angew. Chem. Int. Ed.* **2013**, *52*, 11726–11743. [[CrossRef](#)] [[PubMed](#)]
18. Leow, D.; Li, G.; Mei, T.-S.; Yu, J.-Q. Activation of remote meta-C–H bonds assisted by an end-on template. *Nature* **2012**, *486*, 518–522. [[CrossRef](#)]
19. Lee, S.; Lee, H.; Tan, K.L. Meta-Selective C–H Functionalization Using a Nitrile-Based Directing Group and Cleavable Si-Tether. *J. Am. Chem. Soc.* **2013**, *135*, 18778–18781. [[CrossRef](#)]
20. Negretti, S.; Narayan, A.R.H.; Chiou, K.C.; Kells, P.M.; Stachowski, J.L.; Hansen, D.A.; Podust, L.M.; Montgomery, J.; Sherman, D.H. Directing Group-Controlled Regioselectivity in an Enzymatic C–H Bond Oxygenation. *J. Am. Chem. Soc.* **2014**, *136*, 4901–4904. [[CrossRef](#)]
21. Sambaglio, C.; Schönbauer, D.; Blicke, R.; Dao-Huy, T.; Pototschnig, G.; Schaaf, P.; Wiesinger, T.; Zia, M.F.; Wencel-Delord, J.; Besset, T.; et al. A comprehensive overview of directing groups applied in metal-catalysed C–H functionalisation chemistry. *Chem. Soc. Rev.* **2018**, *47*, 6603–6743. [[CrossRef](#)] [[PubMed](#)]
22. Chen, Z.; Wang, B.; Zhang, J.; Yu, W.; Liu, Z.; Zhang, Y. Transition metal-catalyzed C–H bond functionalizations by the use of diverse directing groups. *Org. Chem. Front.* **2015**, *2*, 1107–1295. [[CrossRef](#)]
23. Xu, Y.; Dong, G. sp<sup>3</sup> C–H activation via exo-type directing groups. *Chem. Sci.* **2018**, *9*, 1424–1432. [[CrossRef](#)]
24. Rej, S.; Ano, Y.; Chatani, N. Bidentate Directing Groups: An Efficient Tool in C–H Bond Functionalization Chemistry for the Expedient Construction of C–C Bonds. *Chem. Rev.* **2020**, *120*, 1788–1887. [[CrossRef](#)] [[PubMed](#)]
25. Zhang, Y.-H.; Shi, B.-F.; Yu, J.-Q. Palladium(II)-Catalyzed ortho Alkylation of Benzoic Acids with Alkyl Halides. *Angew. Chem. Int. Ed.* **2009**, *48*, 6097–6100. [[CrossRef](#)]
26. Dai, H.-X.; Stepan, A.F.; Plummer, M.S.; Zhang, Y.-H.; Yu, J.-Q. Divergent C–H Functionalizations Directed by Sulfonamide Pharmacophores: Late-Stage Diversification as a Tool for Drug Discovery. *J. Am. Chem. Soc.* **2011**, *133*, 7222–7228. [[CrossRef](#)] [[PubMed](#)]
27. Engle, K.M.; Mei, T.-S.; Wasa, M.; Yu, J.-Q. Weak Coordination as a Powerful Means for Developing Broadly Useful C–H Functionalization Reactions. *Acc. Chem. Res.* **2012**, *45*, 788–802. [[CrossRef](#)] [[PubMed](#)]
28. Wang, X.-C.; Hu, Y.; Bonacorsi, S.; Hong, Y.; Burrell, R.; Yu, J.-Q. Pd(II)-Catalyzed C–H Iodination Using Molecular I<sub>2</sub> as the Sole Oxidant. *J. Am. Chem. Soc.* **2013**, *135*, 10326–10329. [[CrossRef](#)]
29. Ma, S.; Villa, G.; Thuy-Boun, P.S.; Homs, A.; Yu, J.-Q. Palladium-Catalyzed ortho-Selective C–H Deuteration of Arenes: Evidence for Superior Reactivity of Weakly Coordinated Palladacycles. *Angew. Chem. Int. Ed.* **2014**, *53*, 734–737. [[CrossRef](#)] [[PubMed](#)]

30. Gandeepan, P.; Ackermann, L. Transient Directing Groups for Transformative C–H Activation by Synergistic Metal Catalysis. *Chem* **2018**, *4*, 199–222. [[CrossRef](#)]
31. Chan, K.S.L.; Wasa, M.; Wang, X.; Yu, J.-Q. Palladium(II)-Catalyzed Selective Monofluorination of Benzoic Acids Using a Practical Auxiliary: A Weak-Coordination Approach. *Angew. Chem. Int. Ed.* **2011**, *50*, 9081–9084. [[CrossRef](#)] [[PubMed](#)]
32. Tran, A.T.; Yu, J.-Q. Practical Alkoxythiocarbonyl Auxiliaries for Iridium(I)-Catalyzed C–H Alkylation of Azacycles. *Angew. Chem. Int. Ed.* **2017**, *56*, 10530–10534. [[CrossRef](#)] [[PubMed](#)]
33. Lu, Y.; Wang, D.-H.; Engle, K.M.; Yu, J.-Q. Pd(II)-Catalyzed Hydroxyl-Directed C–H Olefination Enabled by Monoprotected Amino Acid Ligands. *J. Am. Chem. Soc.* **2010**, *132*, 5916–5921. [[CrossRef](#)]
34. Plata, R.E.; Hill, D.E.; Haines, B.E.; Musaev, D.G.; Chu, L.; Hickey, D.P.; Sigman, M.S.; Yu, J.-Q.; Blackmond, D.G. A Role for Pd(IV) in Catalytic Enantioselective C–H Functionalization with Monoprotected Amino Acid Ligands under Mild Conditions. *J. Am. Chem. Soc.* **2017**, *139*, 9238–9245. [[CrossRef](#)]
35. Mei, T.-S.; Giri, R.; Maugel, N.; Yu, J.-Q. PdII-Catalyzed Monoselective ortho Halogenation of C–H Bonds Assisted by Counter Cations: A Complementary Method to Directed ortho-Lithiation. *Angew. Chem. Int. Ed.* **2008**, *47*, 5215–5219. [[CrossRef](#)] [[PubMed](#)]
36. Yu, Y.; Lv, H.; Li, S. The C–H functionalization of organic cations: An interesting and fresh journey. *Org. Biomol. Chem.* **2020**, *18*, 8810–8826. [[CrossRef](#)]
37. Pototschnig, G.; Maulide, N.; Schnürch, M. Direct Functionalization of C–H Bonds by Iron, Nickel, and Cobalt Catalysis. *Chem. Eur. J.* **2017**, *23*, 9206–9232. [[CrossRef](#)]
38. Sun, X.; Shan, G.; Sun, Y.; Rao, Y. Regio- and Chemoselective C-H Chlorination/Bromination of Electron-Deficient Arenes by Weak Coordination and Study of Relative Directing-Group Abilities. *Angew. Chem. Int. Ed.* **2013**, *52*, 4440–4444. [[CrossRef](#)]
39. Tischler, O.; Kovács, S.; Érsek, G.; Králl, P.; Daru, J.; Stirling, A.; Novák, Z. Study of Lewis acid accelerated palladium catalyzed C–H activation. *J. Mol. Catal. A Chem.* **2017**, *426*, 444–450. [[CrossRef](#)]
40. Vana, J.; Bartacek, J.; Hanusek, J.; Roithová, J.; Sedlak, M. C–H Functionalizations by Palladium Carboxylates: The Acid Effect. *J. Org. Chem.* **2019**, *84*, 12746–12754. [[CrossRef](#)]
41. Fujiwara, Y.; Jia, C. New developments in transition metal-catalyzed synthetic reactions via C–H bond activation. *Pure Appl. Chem.* **2001**, *73*, 319–324. [[CrossRef](#)]
42. Boele, M.D.K.; van Strijdonck, G.P.F.; de Vries, A.H.M.; Kamer, P.C.J.; de Vries, J.G.; van Leeuwen, P.W.N.M. Selective Pd-Catalyzed Oxidative Coupling of Anilides with Olefins through C–H Bond Activation at Room Temperature. *J. Am. Chem. Soc.* **2002**, *124*, 1586–1587. [[CrossRef](#)] [[PubMed](#)]
43. Daugulis, O.; Zaitsev, V.G. Anilide ortho-Arylation by Using C–H Activation Methodology. *Angew. Chem. Int. Ed.* **2005**, *44*, 4046–4048. [[CrossRef](#)] [[PubMed](#)]
44. Brasche, G.; Garcia-Fortanet, J.; Buchwald, S.L. Twofold C–H Functionalization: Palladium-Catalyzed Ortho Arylation of Anilides. *Org. Lett.* **2008**, *10*, 2207–2210. [[CrossRef](#)] [[PubMed](#)]
45. Wang, X.; Mei, T.-S.; Yu, J.-Q. Versatile Pd(OTf)<sub>2</sub>·2H<sub>2</sub>O-Catalyzed ortho-Fluorination Using NMP as a Promoter. *J. Am. Chem. Soc.* **2009**, *131*, 7520–7521. [[CrossRef](#)] [[PubMed](#)]
46. Houlden, C.E.; Hutchby, M.; Bailey, C.D.; Ford, J.G.; Tyler, S.N.G.; Gagné, M.R.; Lloyd-Jones, G.C.; Booker-Milburn, K.I. Room-Temperature Palladium-Catalyzed C–H Activation: Ortho-Carbonylation of Aniline Derivatives. *Angew. Chem. Int. Ed.* **2009**, *48*, 1830–1833. [[CrossRef](#)]
47. Wang, X.; Truesdale, L.; Yu, J.-Q. Pd(II)-Catalyzed ortho-Trifluoromethylation of Arenes Using TFA as a Promoter. *J. Am. Chem. Soc.* **2010**, *132*, 3648–3649. [[CrossRef](#)]
48. Xiao, B.; Gong, T.-J.; Xu, J.; Liu, Z.-J.; Liu, L. Palladium-Catalyzed Intermolecular Directed C–H Amidation of Aromatic Ketones. *J. Am. Chem. Soc.* **2011**, *133*, 1466–1474. [[CrossRef](#)]
49. Shan, G.; Yang, X.; Ma, L.; Rao, Y. Pd-Catalyzed C-H Oxygenation with TFA/TFAA: Expedient Access to Oxygen-Containing Heterocycles and Late-Stage Drug Modification. *Angew. Chem. Int. Ed.* **2012**, *51*, 13070–13074. [[CrossRef](#)]
50. Nishikata, T.; Abela, A.R.; Huang, S.; Lipshutz, B.H. Cationic Palladium(II) Catalysis: C–H Activation/Suzuki-Miyaura Couplings at Room Temperature. *J. Am. Chem. Soc.* **2010**, *132*, 4978–4979. [[CrossRef](#)]
51. Yang, Y.; Yang, X.; Zhang, Y.; Xue, Y. Computational Mechanism Study on Allylic Oxidation of cis-Internal Alkenes: Insight into the Lewis Acid-Assisted Brønsted Acid (LBA) Catalysis in Heteroene Reactions. *J. Org. Chem.* **2018**, *83*, 13344–13355. [[CrossRef](#)]
52. Ghaderi, A.; Iwasaki, T.; Kambe, N. Pivalic Acid-Assisted Rh(III)-Catalyzed C–H Functionalization of 2-Arylpyridine Derivatives Using Arylsilanes. *Asian J. Org. Chem.* **2019**, *8*, 1344–1347. [[CrossRef](#)]
53. Jia, C.; Kitamura, T.; Fujiwara, Y. Catalytic Functionalization of Arenes and Alkanes via C–H Bond Activation. *Acc. Chem. Res.* **2001**, *34*, 633–639. [[CrossRef](#)] [[PubMed](#)]
54. Engle, K.M.; Wang, D.-H.; Yu, J.-Q. Ligand-Accelerated C–H Activation Reactions: Evidence for a Switch of Mechanism. *J. Am. Chem. Soc.* **2010**, *132*, 14137–14151. [[CrossRef](#)] [[PubMed](#)]
55. Labinger, J.A.; Bercaw, J.E. Understanding and exploiting C–H bond activation. *Nature* **2002**, *417*, 507–514. [[CrossRef](#)]
56. Ackermann, L. Carboxylate-Assisted Transition-Metal-Catalyzed C–H Bond Functionalizations: Mechanism and Scope. *Chem. Rev.* **2011**, *111*, 1315–1345. [[CrossRef](#)] [[PubMed](#)]
57. Zhang, S.; Shi, L.; Ding, Y. Theoretical Analysis of the Mechanism of Palladium(II) Acetate-Catalyzed Oxidative Heck Coupling of Electron-Deficient Arenes with Alkenes: Effects of the Pyridine-Type Ancillary Ligand and Origins of the meta-Regioselectivity. *J. Am. Chem. Soc.* **2011**, *133*, 20218–20229. [[CrossRef](#)]

58. Yang, Y.-F.; Cheng, G.-J.; Liu, P.; Leow, D.; Sun, T.-Y.; Chen, P.; Zhang, X.; Yu, J.-Q.; Wu, Y.-D.; Houk, K.N. Palladium-Catalyzed Meta-Selective C–H Bond Activation with a Nitrile-Containing Template: Computational Study on Mechanism and Origins of Selectivity. *J. Am. Chem. Soc.* **2014**, *136*, 344–355. [[CrossRef](#)]
59. Cheng, G.-J.; Yang, Y.-F.; Liu, P.; Chen, P.; Sun, T.-Y.; Li, G.; Zhang, X.; Houk, K.N.; Yu, J.-Q.; Wu, Y.-D. Role of N-Acyl Amino Acid Ligands in Pd(II)-Catalyzed Remote C–H Activation of Tethered Arenes. *J. Am. Chem. Soc.* **2014**, *136*, 894–897. [[CrossRef](#)] [[PubMed](#)]
60. Gorelsky, S.I.; Lapointe, D.; Fagnou, K. Analysis of the Concerted Metalation-Deprotonation Mechanism in Palladium-Catalyzed Direct Arylation Across a Broad Range of Aromatic Substrates. *J. Am. Chem. Soc.* **2008**, *130*, 10848–10849. [[CrossRef](#)] [[PubMed](#)]
61. Potavathri, S.; Pereira, K.C.; Gorelsky, S.I.; Pike, A.; LeBris, A.P.; DeBoef, B. Regioselective Oxidative Arylation of Indoles Bearing N-Alkyl Protecting Groups: Dual C–H Functionalization via a Concerted Metalation-Deprotonation Mechanism. *J. Am. Chem. Soc.* **2010**, *132*, 14676–14681. [[CrossRef](#)]
62. Anand, M.; Sunoj, R.B. Palladium(II)-Catalyzed Direct Alkoxylation of Arenes: Evidence for Solvent-Assisted Concerted Metalation Deprotonation. *Org. Lett.* **2011**, *13*, 4802–4805. [[CrossRef](#)]
63. Gorelsky, S.I.; Lapointe, D.; Fagnou, K. Analysis of the Palladium-Catalyzed (Aromatic)C–H Bond Metalation–Deprotonation Mechanism Spanning the Entire Spectrum of Arenes. *J. Org. Chem.* **2012**, *77*, 658–668. [[CrossRef](#)] [[PubMed](#)]
64. Davies, D.; Macgregor, S.A.; McMullin, C.L. Computational Studies of Carboxylate-Assisted C–H Activation and Functionalization at Group 8–10 Transition Metal Centers. *Chem. Rev.* **2017**, *117*, 8649–8709. [[CrossRef](#)] [[PubMed](#)]
65. Shan, C.; Zhu, L.; Qu, L.-B.; Bai, R.; Lan, Y. Mechanistic view of Ru-catalyzed C–H bond activation and functionalization: Computational advances. *Chem. Soc. Rev.* **2018**, *47*, 7552–7576. [[CrossRef](#)]
66. Geometries were optimized with M06/(LANL2DZ+f; Pd; 6-31G(d); Other atoms). Single-point energies were calculated with M06/(SDD: Pd; 6-311++G(d, p); Other atoms) with the SMD solvation model (dichloroethane was chosen as the solvent). All calculations were performed with Gaussian 09. (Frisch, M.J.; et al.) See SI for more computational details.
67. Skapski, A.C.; Smart, M.L. The crystal structure of trimeric palladium(II) acetate. *J. Chem. Soc. D* **1970**, *11*, b658–b659. [[CrossRef](#)]
68. Kurzeev, S.A.; Kazankov, G.M.; Ryabov, A.D. Second- and inverse order pathways in the mechanism of orthopalladation of primary amines. *Inorg. Chim. Acta* **2002**, *340*, 192–196. [[CrossRef](#)]
69. Bakhmutov, V.I.; Berry, J.F.; Cotton, F.A.; Ibragimov, S.; Murillo, C.A. Non-trivial behavior of palladium(ii) acetate. *Dalton Trans.* **2005**, 1989–1992. [[CrossRef](#)]
70. Gandeepan, P.; Parthasarathy, K.; Cheng, C.-H. Synthesis of Phenanthrone Derivatives from sec-Alkyl Aryl Ketones and Aryl Halides via a Palladium-Catalyzed Dual C–H Bond Activation and Enolate Cyclization. *J. Am. Chem. Soc.* **2010**, *132*, 8569–8571. [[CrossRef](#)] [[PubMed](#)]
71. Yeung, C.S.; Zhao, X.; Borduas, N.; Dong, V.M. Pd-catalyzed ortho-arylation of phenylacetamides, benzamides, and anilides with simple arenes using sodium persulfate. *Chem. Sci.* **2010**, *1*, 331–336. [[CrossRef](#)]
72. Zhao, X.; Yeung, C.S.; Dong, V.M. Palladium-Catalyzed Ortho-Arylation of O-Phenylcarbamates with Simple Arenes and Sodium Persulfate. *J. Am. Chem. Soc.* **2010**, *132*, 5837–5844. [[CrossRef](#)] [[PubMed](#)]
73. Zhou, D.-B.; Wang, G.-W. Synthesis of [60]Fullerene-Fused Tetralones via Palladium-Catalyzed Ketone-Directed sp<sup>2</sup> C-H Activation and sp<sup>3</sup> C-H Functionalization. *Adv. Synth. Catal.* **2016**, *358*, 1548–1554. [[CrossRef](#)]
74. Tóth, B.L.; Kovács, S.; Sályi, G.; Novák, Z. Mild and Efficient Palladium-Catalyzed Direct Trifluoroethylation of Aromatic Systems by C–H Activation. *Angew. Chem. Int. Ed.* **2016**, *55*, 1988–1992. [[CrossRef](#)]
75. Guner, V.A.; Houk, K.N.; Davies, I.W. Computational Studies on the Electrocyclizations of 1-Amino-1,3,5-hexatrienes. *J. Org. Chem.* **2004**, *69*, 8024–8028. [[CrossRef](#)] [[PubMed](#)]
76. Yu, T.-Q.; Fu, Y.; Liu, L.; Guo, Q.-X. How to Promote Sluggish Electrocyclization of 1,3,5-Hexatrienes by Captodative Substitution. *J. Org. Chem.* **2006**, *71*, 6157–6164. [[CrossRef](#)]
77. Xue, L.; Su, W.; Lin, Z. Mechanism of silver- and copper-catalyzed decarboxylation reactions of aryl carboxylic acids. *Dalton Trans.* **2011**, *40*, 11926–11936. [[CrossRef](#)]
78. Ryabov, A.D. Cyclopalladated Complexes in Organic Synthesis. *Synthesis* **1985**, 233–252. [[CrossRef](#)]